



## Exploring the Impact of Preprocessing Techniques on Retinal Blood Vessel Segmentation Using a Study Group Learning Scheme

Bashir, S., Rohail, K., Sadak, F., Hadi, M. U., Muneer, A., Ragab, M. G., Awais, M., & Qureshi, R. (2023). Exploring the Impact of Preprocessing Techniques on Retinal Blood Vessel Segmentation Using a Study Group Learning Scheme. In *2023 IEEE Signal Processing in Medicine and Biology Symposium (SPMB)* (pp. 1-6) Advance online publication. <https://doi.org/10.1109/spmb59478.2023.10372702>

[Link to publication record in Ulster University Research Portal](#)

### Published in:

2023 IEEE Signal Processing in Medicine and Biology Symposium (SPMB)

### Publication Status:

Published online: 29/12/2023

### DOI:

[10.1109/spmb59478.2023.10372702](https://doi.org/10.1109/spmb59478.2023.10372702)

### Document Version

Author Accepted version

### General rights

Copyright for the publications made accessible via Ulster University's Research Portal is retained by the author(s) and / or other copyright owners and it is a condition of accessing these publications that users recognise and abide by the legal requirements associated with these rights.

### Take down policy

The Research Portal is Ulster University's institutional repository that provides access to Ulster's research outputs. Every effort has been made to ensure that content in the Research Portal does not infringe any person's rights, or applicable UK laws. If you discover content in the Research Portal that you believe breaches copyright or violates any law, please contact [pure-support@ulster.ac.uk](mailto:pure-support@ulster.ac.uk).

# Exploring The Impact of Pre-processing Techniques on Retinal Blood Vessel Segmentation using Study Group Learning Scheme

S. Bashir<sup>1</sup>, K. Rohail<sup>1</sup>, F. Sadak<sup>2</sup>, M.U. Hadi<sup>3</sup>, A. Muneer<sup>1</sup>, M.G. Ragab<sup>5</sup>, M. Awais<sup>4</sup> and R. Qureshi<sup>1</sup>

1. Fast School of Computing, National University of Computer and Emerging Sciences, Karachi Campus, Pakistan
  2. Department of Mechanical Engineering, Bartin University, Turkey
  3. School of Engineering, Ulster University, Belfast, United Kingdom
  4. Department of Imaging Physics, MD Anderson Cancer Center, The University of Texas, Houston, Texas, Houston, USA
  5. Department of Computer and Information Sciences, Universiti Teknologi PETRONAS Seri Iskandar, Malaysia
- {k201366, k201312, rizwan.qureshi}@nu.edu.pk, ferhat.sadak@gmail.com, muneeramgad@gmail.com, mogragab@gmail.com, m.awais0100@gmail.com

**Abstract**— The segmentation of retinal vessels in retinal images is vital for automated diagnosis of retinal diseases. This is a challenging task because it requires accurate manual labeling of the vessels by expert clinicians and the detection of tiny vessels is difficult due to limited samples, low contrast, and noise. In this study, we explore the use of pre-processing techniques such as contrast-limited adaptive histogram equalization (CLAHE), grad-cam analysis and min-max contrast stretching to improve the performance of a study-group learning (SGL) segmentation model. We evaluate the impact of these pre-processing techniques on the accuracy, sensitivity, specificity, AUC, IoU, and Dice scores using four publicly available datasets, DRIVE, CHASE, HRF and IOSTAR. Our findings indicate that the utilization of the Min- Max technique resulted in a notable enhancement in the accuracy of both the DRIVE and CHASE datasets, with an approximate increase of 3% and 2% respectively. Conversely, the impact of the CLAHE method was discernible solely in the DRIVE dataset, demonstrating an improvement in accuracy of 1%. In addition, our results demonstrated superior accuracy performance for both the DRIVE and CHASE datasets compared to the findings of the reviewed studies. The GitHub repo for this project is available at Link.

**Keywords**— Study Group Learning, Vessel Segmentation, Medical Imaging, CLAHE, Min Max Contrast Stretching, Grad-Cam

## I. INTRODUCTION

Any abnormality in the retina or ocular condition, such as glaucoma or diabetic retinopathy, can impair a person's vision. Glaucoma is the second leading cause of irreversible vision loss worldwide, after cataracts [1]. Approximately 12% of all cases of blindness worldwide can be attributed to retinal abnormalities. The structure of retinal blood vessels is critical for the diagnosis of such abnormalities. The identification and localization of retinal vessels enable the differentiation of the diverse vasculature structure of the retina from the background of the fundus image. This allows clinicians to interpret potentially problematic retinal anatomical structures such as abnormal lesions, macula, and optic disc [2–

4]. Even the color of the retina changes throughout life and can be used as a biomarker for a variety of diseases, including diabetes and stroke prediction [2–4].

Deep learning is the state-of-the-art in many computer vision problems, including medical imaging [5, 6]. The evolution of deep learning has led to the development of automated models for more accurate and precise segmentation of retinal blood vessels. These models are instrumental in aiding the clinical application of retinal blood vessel segmentation. They are capable of initially segmenting the vessels and then extracting features that correlate with specific retinal abnormalities. Existing literature suggests the implementation of Convolutional Neural Networks (CNNs) based approaches, such as U-Net [7], and Fully Convolutional Neural Networks for vessel segmentation [8]. Data augmentation techniques have been shown to improve the segmentation results of these models significantly [9].

Other studies have shown remarkable segmentation results for retinal vessel segmentation using various models such as RV-GAN, a new multi-scale generative architecture, with 98.87% accuracy [10], DUNet, a deformable network, with 97.22% [11] on STARE dataset. Another study proposed the Contextual Multi-Scale Multi-Level Network (CMM-Net) for segmenting retinal blood vessels giving the DICE score of 80.27% [1] which is a relatively successful model in contrast to PSPNet and DeepLabv3 models on thin vessels. The main logic of their research is to combine global contextual features from multiple spatial scales at each contracting convolutional network level in the U-Net.

In another study, a residual convolution neural network was proposed to segment vessel structure along with stems and terminals [12]. It achieved an average accuracy of 95.90% and 96.88% on DRIVE and STARE datasets. The algorithm proved to be an efficient method for detecting more detailed capillaries. To learn local and global blood vessels, Graph Neural Network

was integrated with CNN architecture proposing Vessel Graph Network (VGN) for modeling the graphical retinal vessel structure. The model not only enhances the connection between weak and strong vessels but also covers up the false positive cases [13].

In this paper, we employed the Study Group Learning (SGL) model [14] as the base framework on four vessel datasets: DRIVE, CHASE, IOSTAR and HRF [15]. It should be noted that the available datasets are highly imbalanced [16, 17], implying that the ratio of thick and thin vessels is unavoidably high. As a result, the available models inevitably focus on thick vessels rather than thin vessels. To address this problem, our research will include a comprehensive analysis of preprocessing techniques to highlight thin vessels in order to learn the discriminative features, while also making explicit its explainable model structure [18]. GRAD-CAM is used for the visualization of features and improve the explainability of the model. Moreover, in this paper, we have not included any augmentation, as we aimed to do work on the real images, and just want to observe the effects of pre-processing methods.

## II. RESEARCH METHODOLOGY

### II-A. Datasets

In this study, the proposed models being implemented are based on SGL model on four datasets, namely DRIVE, CHASE, HRF and IOSTAR. The detail of the dataset is shown in Table 1. All datasets consist of raw retinal images and vessel label mask for training as well as testing.

### II-B. Description of the SGL Model

The provided baseline model structure used for our study is depicted in Figure 1. The model uses a concatenated UNet architecture, which comprises an encoder and a corresponding decoder. The encoder encodes the input image features into a compact representation, while the decoder reconstructs the segmentation map from the encoded features. This architecture enables accurate vessel segmentation by allowing the model to gather both local and global context information. The SGL model technique combines modules for segmentation and enhancement to produce segmentation maps while simultaneously learning how to improve retinal images. In contrast to earlier methods, this model uses the raw recorded images without any pre-processing

techniques to preserve all of the information that is present in the retinal images.

In particular, a three-channel raw retinal image with the symbol  $I$  serves as the model's input. The goal of processing this image is to increase its contrast and highlight the vessel structures, producing an improved image denoted as  $I_e$ . The model also seeks to estimate the segmentation map  $I_c$ , which represents the vessels identified by qualified healthcare professionals and is used as the ground truth source. It is important to note that the enhanced image  $I_e$  keeps the majority of the image's information, including retinal texturing and vessels. When examining the segmentation outcomes  $I_c$ , this feature helps doctors better comprehend and interpret the performance of the learned model.

### II-C. Preprocessing Techniques

We have used two preprocessing techniques for retinal image enhancement, CLAHE and MIN-MAX contrast stretching.

#### II-C1. CLAHE

CLAHE is a widely used image enhancement technique that aims to improve the local contrast in an image while limiting the amplification of noise. It performs this by dividing the image into small regions called tiles and performing histogram equalization on each tile independently. By locally redistributing the pixel intensities within each tile, CLAHE enhances the local contrast and brings out details that may be obscured by low contrast or uneven illumination. In more detail, the steps involved in the implementation of this method can be listed below [19]:

- Initiates region size and clip limit with histogram shape for each region. The clip limit of a histogram is computed by following Equation 1:

$$\beta = \frac{M}{N}(1 + \alpha * 100 * (S_{max} + 1)) \quad (1)$$

Where  $M$  is region size,  $N$  is grey-scale value-256 and  $\alpha$  is clip factor that refers to addition of a histogram between a range of 0-100.

- Cuts the histogram using value of clip limit.
- Then the highest value of clip limit referred as excess is used for distributing to obtain new histogram that is further mapped over original image.
- The resulting image is generated via pixel interpolation in neighbored regions.

#### II-C2. MIN MAX Contrast Stretching

A key preprocessing method used in image analysis and enhancement to enhance an image's contrast and

Table 1. Dataset Information

Datasets	Train Images	Test Images
Drive	20	20
CHASE	20	8
HRF	15	30
IOSTAR	18	18

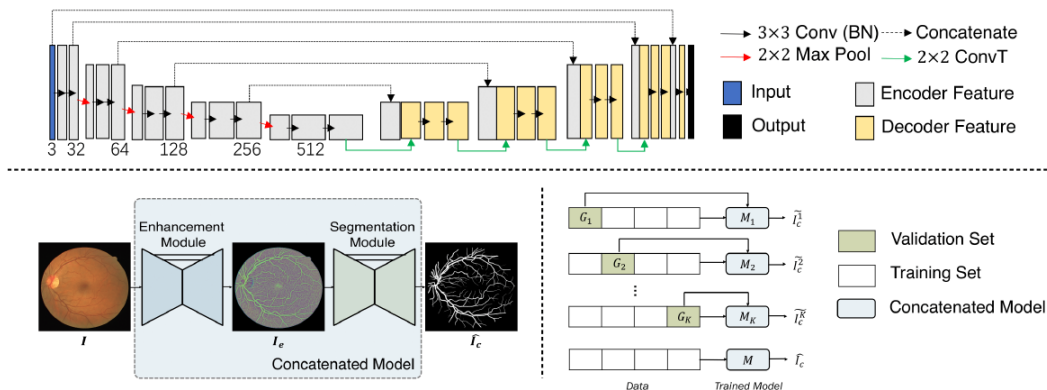


Figure 1. Fig. 1. Illustration of the SGL framework [14]

dynamic range is called min-max stretching, also known as intensity normalization. The goal of this technique is to increase the range of intensities and enhance the ability to perceive details by taking into account the minimum (lower) and maximum (higher) intensity values that are present in the image.

In Min-Max stretching, the upper intensity value is mapped to the highest representable value, frequently 255, in an 8-bit grayscale image, while the lower intensity value is mapped to 0. The whole intensity range is used effectively thanks to this linear translation. To keep the transformation function monotonic and linear, the intermediate intensity values must be appropriately changed.

To calculate the new intensity values during Min-Max stretching, a formula based on linear interpolation is used. This formula is applied to each pixel in the image, and it can be represented by the following equation 2.

$$X_{new} = \frac{X_{input} - X_{min}}{X_{max} - X_{min}} * 255 \quad (2)$$

The intermediate intensity values are linearly scaled and modified to fit inside the specified dynamic range by using Equation 2. By doing this, it is guaranteed that the image's overall contrast will be improved while maintaining the relative connections between intensities.

### III. RESULTS AND DISCUSSION

In this section, we provide the outcomes of our implementation and discussion of our study on the impact of preprocessing techniques on retinal blood vessel segmentation using the SGL scheme. This section provides a detailed analysis of the experimental results obtained by applying various preprocessing techniques on retinal images using deep learning models for segmentation on publicly available datasets, namely HRF, DRIVE,

CHASE and IOSTAR. The section also includes a thorough discussion of the results, highlighting the effectiveness of different pre-processing techniques in improving the accuracy and efficiency of retinal blood vessel segmentation. Additionally, we compare our results with the state-of-the-art approaches and highlight the advantages of our proposed approach. Initially, in order to assess the impact of preprocessing techniques, namely CLAHE and Min-Max stretching, each dataset was subjected to these techniques. The resulting datasets were then evaluated using an SGL model under three conditions: without any preprocessing, with preprocessing using CLAHE, and with preprocessing using Min-Max stretching. The purpose of this evaluation was to compare the performance of the segmentation model under different preprocessing scenarios.

#### III-A. Performance evaluation of CLAHE and Min-Max Stretching

In this section, we evaluate the impact of the implemented pre-processing techniques on retinal blood vessel segmentation using an SGL scheme. We employ commonly used evaluation metrics, including accuracy, sensitivity, specificity, AUC, background IoU, Vessel IoU, and dice score, to ensure a fair comparison between the employed models. The experimental results demonstrating the effect of pre-processing techniques are provided in Table 3. The performance of pre-processing techniques is highly dependent on the histogram of the image, which influences its effectiveness. Consequently, the effects of the CLAHE and Min-Max stretching techniques were not generalized across all datasets used in our study. Specifically, the impact of the Min-Max technique was not significant on the HRF and IOSTAR datasets. However, we observed that the Min-Max technique increased the accuracy of the DRIVE and CHASE datasets by approximately 3% and 2%, respectively. On the other hand, the CLAHE method's

effect was only observable on the DRIVE dataset, where it improved the accuracy by 1%.

Overall, the effectiveness of the preprocessing techniques is highly dependent on the dataset used, as it is closely tied to the image quality. Therefore, it is crucial to optimize the preprocessing techniques specifically for the images employed in the segmentation task. This optimization process has proven to be valuable, as it enhances the accuracy of the segmentation models. The results indicate that tailoring the pre-processing techniques to the characteristics of the dataset and image quality can yield substantial improvements in segmentation accuracy. This finding emphasizes the importance of considering dataset-specific preprocessing optimizations in retinal blood vessel segmentation tasks. By doing so, researchers and practitioners can achieve more accurate and reliable results, which are crucial in the field of medical image analysis. In overall, the results and analysis presented in this section highlight the significant impact of pre-processing techniques on retinal blood vessel segmentation task, particularly for the segmentation of the thin vessels where the accuracy is mostly sacrificed.

### III-B. GRAD-CAM analysis on the performance of retinal thin vessels

In this study, the performance of the Gradcam method was evaluated using several performance metrics on four different datasets: HRF, DRIVE, CHASE, and IOSTAR. The Grad-cam results for each dataset are depicted in Figure 2. The results in Table 2 demonstrated that the Gradcam method achieved noteworthy accuracy on all datasets, with a range of 0.821 to 0.974. The sensitivity scores ranged from 0.66 to 0.916 indicating that the Gradcam method is effective in detecting positive cases in all four datasets. The specificity scores were also high, ranging from 0.984 to 0.994, indicating that the Gradcam method is able to accurately identify negative cases as well. In terms of vessel IoU, the HRF dataset achieved the highest score of 0.891, followed by the DRIVE dataset with 0.72. The CHASE and IOSTAR datasets had lower scores of 0.531 and 0.875, respectively. Finally, the dice scores, which are another measure of segmentation accuracy, ranged from 0.796 to 0.891, with the highest score achieved on the DRIVE dataset. Lastly, the results suggest that the Gradcam method is effective in accurately segmenting blood vessels in retinal fundus images. The method

Table 2. Performance Comparison

Performance Metrics	HRF	Drive	CHASE	IOSTAR
Accuracy	0.974	0.887	0.821	0.927
Sensitivity	0.916	0.66	0.907	0.852
Specificity	0.994	0.984	0.992	0.992
Vessel <sub>IoU</sub>	0.891	0.72	0.531	0.875
Dice	0.891	0.796	0.873	0.821

can be particularly useful for detecting and diagnosing retinal diseases, such as diabetic retinopathy and age-related macular degeneration. However, further studies are needed to evaluate the performance of the Gradcam method on larger and more diverse datasets. The aim of including grad-cam analysis in our study to also separately evaluate the grad-cam results' effect on segmentation accuracy while demonstrating the explainability structure of the SGL model.

Table 3. Comparison of SGL model on four public datasets

Datasets	Metrics	SGL	CLAHE	Min-Max
HRF	Accuracy	0.9698	0.8802	0.9620
	Sensitivity	0.8566	0.7625	0.9154
	Specificity	0.9787	0.9441	0.9680
	AUC	0.9880	0.9812	0.9964
	Background_IoU	0.9677	0.8521	0.9604
	Vessel_IoU	0.6797	0.5741	0.6094
	Dice	0.8079	0.7187	0.7225
DRIVE	Accuracy	0.9659	0.9702	0.9987
	Sensitivity	0.8817	0.7927	0.6488
	Specificity	0.9738	0.9952	0.9996
	AUC	0.9883	0.9682	0.9991
	Background_IoU	0.9632	0.9685	0.9987
	Vessel_IoU	0.6862	0.7215	0.5001
	Dice	0.8134	0.8188	0.6412
CHASE	Accuracy	0.9716	0.9716	0.9908
	Sensitivity	0.9056	0.9056	0.8819
	Specificity	0.9761	0.9761	0.9979
	AUC	0.9906	0.9906	0.9986
	Background_IoU	0.9699	0.9699	0.9905
	Vessel_IoU	0.6681	0.6681	0.3352
	Dice	0.8003	0.8003	0.4572
IOSTAR	Accuracy	0.9705	0.8517	0.9621
	Sensitivity	0.8899	0.8253	0.7293
	Specificity	0.9794	0.9536	0.9871
	AUC	0.9873	0.9748	0.9986
	Background_IoU	0.9675	0.8175	0.9607
	Vessel_IoU	0.7523	0.5796	0.4937
	Dice	0.8535	0.7192	0.6347

### III-C. Comparison of our work with literature

Table 4 presents a comparative analysis of various studies that have evaluated the performance of deep learning models for the task of retinal vessel segmentation. The evaluation metrics used in these studies include precision, sensitivity, specificity, accuracy, and area under the curve (AUC). Our comparative analysis includes a variety of datasets employed in various studies. As depicted in Table 4, the highest accuracy for HRF dataset was achieved by Wu et al. [20] with an accuracy of 0.9842. They also achieved the highest accuracy for IOSTAR dataset with an accuracy of 0.9865. The highest accuracy for the DRIVE dataset was obtained by Jiang et al. [21] which is 0.9864. On the other hand, the highest accuracy for CHASE dataset was achieved by Guo et al. [22] which is 0.9872. In comparison to our work on the effect of pre-processing techniques on the accuracy of the retinal vessel segmentation in the literature, it offers more accurate results for certain datasets. For instance, particularly Min-Max stretching technique helped the SGL model to learn better the segmentation of the thin vessels. Although the accuracy was not improved remarkably

for HRF and IOSTAR datasets, our proposed model obtained 0.9987 and 0.9908 accuracy for DRIVE and CHASE dataset, which clearly demonstrate the effect of the pre-processing technique on the segmentation of retinal vessel outcome. Hence, our results outperformed in terms of accuracy for DRIVE and CHASE dataset compared to the reviewed studies. The limitation of our work is that it evaluated the impact of the pre-processing methods on only four publicly available datasets. While the datasets were diverse and included images from different sources, they may not represent the full range of retinal images. The findings may not be generalizable to other datasets with different characteristics, such as varying image quality or different types of retinal diseases. Additionally, the study did not use any private or newly acquired datasets, which may have provided more insight into the performance of the pre-processing techniques.

The performance of the reviewed models can be significantly improved by using appropriate preprocessing techniques to enhance the quality of retinal images. Several preprocessing techniques have been proposed in the literature, including contrast enhancement, noise reduction, vessel enhancement, and morphological operations. These techniques can be applied either individually or in combination to obtain better results. However, the choice and combination of preprocessing techniques depend on the specific dataset and deep learning model used for segmentation. This approach can help identify the most effective preprocessing techniques for retinal vessel segmentation and facilitate their translation to clinical practice.

#### IV. CONCLUSION AND FUTURE WORK

In conclusion, retinal vessel segmentation using retinal images is essential for the development of automatic diagnostic models for the diagnosis of retinal diseases. This research paper explored the impact of preprocessing techniques, such as CLAHE and min-max contrast stretching, on a study group learning (SGL) segmentation model. The study demonstrated that preprocessing techniques can significantly improve the accuracy of the SGL model in identifying and classifying tiny retinal blood vessels. The results indicate that the min-max normalization technique is the most effective preprocessing method for this task within the scope of our work. The findings of this study have important implications for the development of accurate and efficient diagnostic models for retinal diseases. In the future, it will be interesting to see the performance of large language models for vessel segmentation task [23].

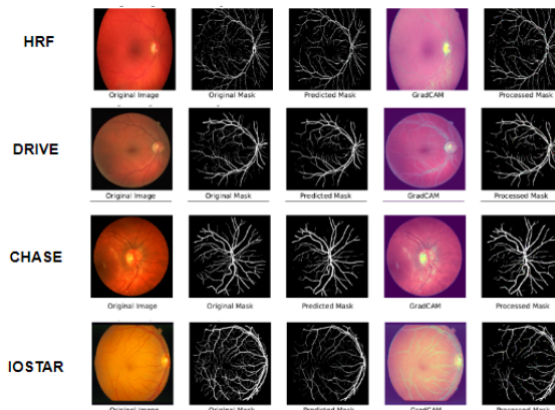


Figure 2. GRAD-CAM analysis results on HRF, CHASE, DRIVE and IOSTAR datasets

Table 4. Comparison of U-net like models proposed in the literature

Reference	Database	Precision	Sensitivity	Specificity	Accuracy	AUC
[20]	DRIVE	NA	0.8289	0.9838	0.9697	0.9837
	CHASE	NA	0.8365	0.9839	0.9744	0.9867
	IOSTAR	NA	0.8255	0.9830	0.9706	0.9865
	HRF	NA	0.8114	0.9823	0.9687	0.9842
[11]	DRIVE	0.8529	0.7963	0.9800	0.9566	0.9802
	CHASE	0.7630	0.8155	0.9752	0.9610	0.9804
	HRF	0.8593	0.7464	0.9874	0.9651	0.9831
[24]	DRIVE	NA	0.83	0.984	0.968	0.978
[25]	DRIVE	NA	0.7614	0.9837	0.9604	0.9846
	CHASE	NA	0.7993	0.9868	0.9783	0.9869
[21]	DRIVE	NA	0.7839	0.989	0.9709	0.9864
	CHASE	NA	0.7839	0.9894	0.9721	0.9866
[26]	DRIVE	NA	0.7941	0.9798	0.9558	0.9847
	CHASE	NA	0.8167	0.9704	0.9608	0.9865
[27]	DRIVE	NA	0.7921	0.9810	0.9568	0.9806
	CHASE	NA	0.7818	0.9819	0.9635	0.9810
	IOSTAR	NA	0.7322	0.9802	0.9544	0.9623
[28]	DRIVE	NA	0.7653	0.9818	0.9542	NA
	CHASE	NA	0.7633	0.9809	0.9610	NA
	HRF	0.6647	0.7881	0.9592	0.9437	NA
[22]	DRIVE	0.8335	0.7891	0.9848	0.9674	0.9836
	CHASE	0.8486	0.7559	0.9900	0.9738	0.9872
[29]	DRIVE	NA	0.7991	0.9813	0.9581	0.9823
	CHASE	NA	0.8239	0.9813	0.9670	0.9871
	IOSTAR	NA	0.7538	0.9893	0.9652	0.9859
	HRF	NA	0.7803	0.9843	0.9654	0.9837

#### REFERENCES

- [1] S. Kingman, "Glaucoma is second leading cause of blindness globally," *Bulletin of the World Health Organization*, vol. 82, pp. 887–888, 2004.
- [2] C. Köse, C. İki *et al.*, "A personal identification system using retinal vasculature in retinal fundus images," *Expert Systems with Applications*, vol. 38, no. 11, pp. 13 670–13 681, 2011.
- [3] G. Lim, Z. W. Lim, D. Xu, D. S. Ting, T. Y. Wong, M. L. Lee, and W. Hsu, "Feature isolation for hypothesis testing in retinal imaging: an ischemic stroke prediction case study," *Proceedings of the AAAI Conference on Artificial Intelligence*, vol. 33, no. 01, 2019, pp. 9510–9515.
- [4] N. Salamat, M. M. S. Missen, and A. Rashid, "Diabetic retinopathy techniques in retinal images: A review," *Artificial intelligence in medicine*, vol. 97, pp. 168–188, 2019.

- [5] M. U. Hadi, R. Qureshi, A. Ahmed, and N. Iftikhar, "A lightweight corona-net for covid-19 detection in x-ray images," *Expert Systems with Applications*, vol. 225, p. 120023, 2023.
- [6] R. Qureshi, M. Irfan, H. Ali, A. Khan, A. S. Nittala, S. Ali, A. Shah, T. M. Gondal, F. Sadak, Z. Shah *et al.*, "Artificial intelligence and biosensors in healthcare and its clinical relevance: A review," *IEEE Access*, 2023.
- [7] S. A. David, C. Mahesh, V. D. Kumar, K. Polat, A. Alhudhaif, and M. Nour, "Retinal blood vessels and optic disc segmentation using u-net," *Mathematical Problems in Engineering*, vol. 2022, pp. 1–11, 2022.
- [8] A. Oliveira, S. Pereira, and C. A. Silva, "Retinal vessel segmentation based on fully convolutional neural networks," *Expert Systems with Applications*, vol. 112, pp. 229–242, 2018.
- [9] E. S. Uysal, M. Ş. Bilici, B. S. Zaza, M. Y. Özgenç, and O. Boyar, "Exploring the limits of data augmentation for retinal vessel segmentation," *arXiv preprint arXiv:2105.09365*, 2021.
- [10] S. A. Kamran, K. F. Hossain, A. Tavakkoli, S. L. Zuckerbrod, K. M. Sanders, and S. A. Baker, "Rv-gan: Segmenting retinal vascular structure in fundus photographs using a novel multi-scale generative adversarial network," *Medical Image Computing and Computer Assisted Intervention—MICCAI 2021: 24th International Conference, Strasbourg, France, September 27–October 1, 2021, Proceedings, Part VIII 24*. Springer, 2021, pp. 34–44.
- [11] Q. Jin, Z. Meng, T. D. Pham, Q. Chen, L. Wei, and R. Su, "Dunet: A deformable network for retinal vessel segmentation," *Knowledge-Based Systems*, vol. 178, pp. 149–162, 2019.
- [12] S. Xu, Z. Chen, W. Cao, F. Zhang, and B. Tao, "Retinal vessel segmentation algorithm based on residual convolution neural network," *Frontiers in Bioengineering and Biotechnology*, vol. 9, p. 786425, 2021.
- [13] S. Y. Shin, S. Lee, I. D. Yun, and K. M. Lee, "Deep vessel segmentation by learning graphical connectivity," *Medical image analysis*, vol. 58, p. 101556, 2019.
- [14] Y. Zhou, H. Yu, and H. Shi, "Study group learning: Improving retinal vessel segmentation trained with noisy labels," *Medical Image Computing and Computer Assisted Intervention—MICCAI 2021: 24th International Conference, Strasbourg, France, September 27–October 1, 2021, Proceedings, Part I 24*. Springer, 2021, pp. 57–67.
- [15] A. Sarhan, J. Rokne, R. Alhaji, and A. Crichton, "Transfer learning through weighted loss function and group normalization for vessel segmentation from retinal images," *2020 25th International Conference on Pattern Recognition (ICPR)*. IEEE, 2021, pp. 9211–9218.
- [16] H. Kaur, H. S. Pannu, and A. K. Malhi, "A systematic review on imbalanced data challenges in machine learning: Applications and solutions," *ACM Computing Surveys (CSUR)*, vol. 52, no. 4, pp. 1–36, 2019.
- [17] M. Awais, H. Ghayvat *et al.*, "Face and its features detection during nap," *2018 IEEE 23rd International Conference on Digital Signal Processing (DSP)*. IEEE, 2018, pp. 1–5.
- [18] A. R. Bhatt, R. Vaghashiya, M. Kulkarni, and D. P. Kamaraj, "Explainable artificial intelligence in retinal imaging for the detection of systemic diseases," *arXiv preprint arXiv:2212.07058*, 2022.
- [19] F. Hana and I. Maulida, "Analysis of contrast limited adaptive histogram equalization (clahe) parameters on finger knuckle print identification," *Journal of Physics: Conference Series*, vol. 1764, no. 1. IOP Publishing, 2021, p. 012049.
- [20] H. Wu, W. Wang, J. Zhong, B. Lei, Z. Wen, and J. Qin, "Scs-net: A scale and context sensitive network for retinal vessel segmentation," *Medical Image Analysis*, vol. 70, p. 102025, 2021.
- [21] Y. Jiang, N. Tan, T. Peng, and H. Zhang, "Retinal vessels segmentation based on dilated multi-scale convolutional neural network," *Ieee Access*, vol. 7, pp. 76 342–76 352, 2019.
- [22] C. Guo, M. Szemenyei, Y. Pei, Y. Yi, and W. Zhou, "Sd-unet: A structured dropout u-net for retinal vessel segmentation," *2019 IEEE 19th International Conference on Bioinformatics and Bioengineering (BIBE)*. IEEE, 2019, pp. 439–444.
- [23] M. U. Hadi, R. Qureshi, A. Shah, M. Irfan, A. Zafar, M. Shaikh, N. Akhtar, J. Wu, and S. Mirjalili, "A survey on large language models: Applications, challenges, limitations, and practical usage," *TechRxiv*, 2023.
- [24] D. Wang, G. Hu, and C. Lyu, "Frnet: an end-to-end feature refinement neural network for medical image segmentation," *The Visual Computer*, vol. 37, pp. 1101–1112, 2021.
- [25] P. Yin, R. Yuan, Y. Cheng, and Q. Wu, "Deep guidance network for biomedical image segmentation," *IEEE access*, vol. 8, pp. 116 106–116 116, 2020.
- [26] Y. Lv, H. Ma, J. Li, and S. Liu, "Attention guided u-net with atrous convolution for accurate retinal vessels segmentation," *IEEE Access*, vol. 8, pp. 32 826–32 839, 2020.
- [27] X. Li, Y. Jiang, M. Li, and S. Yin, "Lightweight attention convolutional neural network for retinal vessel image segmentation," *IEEE Transactions on Industrial Informatics*, vol. 17, no. 3, pp. 1958–1967, 2020.
- [28] Z. Yan, X. Yang, and K.-T. Cheng, "Joint segment-level and pixel-wise losses for deep learning based retinal vessel segmentation," *IEEE Transactions on Biomedical Engineering*, vol. 65, no. 9, pp. 1912–1923, 2018.
- [29] D. Wang, A. Haytham, J. Pottenburgh, O. Saeedi, and Y. Tao, "Hard attention net for automatic retinal vessel segmentation," *IEEE Journal of Biomedical and Health Informatics*, vol. 24, no. 12, pp. 3384–3396, 2020.